TELKOMNIKA Indonesian Journal of Electrical Engineering
Vol.12, No.7, July 2014, pp. 5613 ~ 5620
DOI: 10.11591/telkomnika.v12i7.5739

Detecting Rice Growth Using ALOS Multispectral and Synthetic Aperture Radar

Bambang H. Trisasongko*, Dyah R. Panuju, La Ode S. Iman
Department of Soil Science and Land Resource, Bogor Agricultural University,
Jalan Meranti, Dramaga, Bogor 16680, Indonesia,
Phone/Fax: +62 2518422325
*Corresponding author, e-mail: trisasongko@live.it

Abstract

Rice monitoring is a substantial to Asian countries, including Indonesia, since most inhabitants consume rice on a daily basis. As field survey requires substantial time and budget, one relies on remotely sensed data, especially taken through spaceborne platform. This research discusses multispectral and linearly polarized Synthetic Aperture Radar (SAR) from Advanced Land Observing Satellite and their applications to observe various rice growth information. It appears that both sensors provided useful rice growth data leading to the possibility on improving rice field information extraction. Classification scheme by means of Random Forest suggested that both data were fairly acceptable for timely monitoring.

Keywords*: decision tree, multispectral, radar, random forest, rice*

1. Introduction

Rice is a staple food for Indonesians. Although the demand tends to increase, rice has been planted in very few locations in Indonesia. Java has been serving as primary production center for the country since early 1900s [1]. This has been supported by suitable land resources, water availability and thorough irrigation networks [2]. Monitoring of rice can be established by field surveys or through remote sensing. In many cases, combining both approaches has been the most reliable. Optical remotely-sensed data have been serving as primary datasets. Nonetheless, clouds are persistent in many areas, where complementary data are then required. An alternative to this situation is Synthetic Aperture Radar (SAR) data.

SAR data have been studied for rice monitoring considerably. Scientific literature tends to exploit more on C-band SARs, probably due to their continuous data supply since the era of ERS-1/SAR Advanced Microwave Imager in 1980s-1990s. Haldar and Patnaik [3], for instance, studied C-band Radarsat-1 coupled with AWiFS data to monitor Indian *rabi* rice. Another study in China [4] reported that C-band Envisat ASAR data successfully estimated leaf area index (LAI).

L-band SAR was exploited as well, although in a lesser extent. Japan was the only L-band SAR provider operating JERS-1/SAR at first and later ALOS Phased-Array L-Band SAR (PALSAR). Ishitsuka [5] presented a rice field observation in Japan using PALSAR single, dual and fully polarimetry. The research indicated that observation of Japanese small-scale rice field was quite unsuccessful, although the use of fully polarimetry was promising. Using dual polarized PALSAR data, Ling *et al*. [6] found that mapping rice fields in China was possible. Those research suggest that fully polarimetric SAR may overcome limitation in rice paddy monitoring, despite very limited scene coverage. In addition, multitemporal analysis using single or dual linearly polarized data has been favorable. Wang *et al*. [7] for example, relied on PALSAR multitemporal observation to study characteristics of Southeast China rice fields. The report of Ishitsuka [5] pioneered PALSAR fully polarimetric implementation in rice fields. Nonetheless, literature reviews suggested that there have been a few, if any, reports on the comparison of multispectral and fully polarimetric SAR data for rice field monitoring in tropical regions.

Anticipating near future launch of PALSAR-2, this paper presents a study of SAR data analysis to obtain thematic map of rice growth, in comparison with multispectral dataset. To

Received January 4, 2014; Revised March 16, 2014; Accepted April 6, 2014

extend Ishitsuka's work [5], we employed PALSAR fully polarimetric data to observe their performance in an Indonesian test site.

2. Research Method

The research was located on rice fields managed by PT Sang Hyang Seri (SHS), a state enterprise responsible supplying rice seedling. Planted rice varieties include Sintanur, Bengawan and Ciherang. The latter has been popular in Indonesia and therefore selected as the only variety in our analysis. The area covering about 3,100 ha was located in Subang Regency, West Java (Figure 1).

Figure 1. Research Location

Rice is planted in blocks. A block occupies about 5-18 Ha with similar width of 200m. A group of blocks is managed by a sector manager. Transplanting by means of conventional (non-mechanical) way is usually accomplished within 4-7 days for each block. This leads to variability of rice growing phase within site location, and allows continuation of rice supply to the seed plant. A typical distance between plants is 20cm.

During the research, several datasets were collected. ALOS AVNIR-2 data were obtained from KKP3T project, acquired in 2008 and 2009. ALOS PALSAR fully polarimetric (PLR) datasets consist of 2007, 2009 and 2010 data. The 2010 PLR data are a subject of future investigation and are not being reported in this paper.

In order to extend the analysis, additional datasets were acquired. A scene of ALOS PRISM was obtained to construct baseline thematic dataset in GIS software based on data fusion with AVNIR-2. Four algorithms were evaluated, however, Intensity-Hue-Saturation (IHS) [8] product was selected (Figure 2) to map rice fields. Additional datasets including baseline maps were obtained from BAKOSURTANAL.

Most of datasets to assist the analysis were collected *in situ*. Field surveys were conducted during the 2009 and 2010 dry seasons, and additionally in 2011 (wet season). Based on the preliminary information provided by the company, sample blocks were selected. On those blocks, several measurements were taken, including averaged height and ground moisture condition (dry, wet or flooded).

All ALOS images were provided by Japan Aerospace Exploration Agency (JAXA) in standard CEOS format. These data were then pre-processed using ASF MapReady 2.3.17 to retrieve the digital number (DN). This format is not recommended for biophysical analysis, therefore computation of radiance was then performed using following equation:

$$L = \frac{1}{R}\left\{(O - B_a - B_{NL} - C) - (B - B_a^{'} - C^{'})\right\} \quad (1)$$

Where
L : radiance (W/m2.sr.μm)
R : sensitivity
O : signal output digital value
C : dummy pixel output mean

B_a : offset of exposure
B_{NL} : non-linear offset
B : output digital value – dark
C' : dummy pixel output – dark
B_a' : offset of exposure – dark

Figure 2. A Subset of HSV Data to Construct Rice Field Map, AVNIR data © JAXA

Based on the equation, radiance data were obtained and subsequently fed into NDVI analysis. Precisely 75 pixels were sampled for each date to observe variability of NDVI across research location.

For comparison, two PALSAR PLR scenes were studied in this research. The PLR mode preserves original radar measurement and represented in complex number (known as Single Look Complex, SLC). The following equation was employed to derive backscatter coefficient of respective polarization [9]

$$\sigma^0 = 10 \cdot \log_{10}\left\langle I^2 + Q^2 \right\rangle + CF - A \quad (2)$$

Where I and Q respectively represents real and imaginary part of SLC data. Conversion factor A was derived using a model [9] which is 32.0. Meanwhile, calibration factor CF value was -83 dB, as suggested by previous calibration study conducted by JAXA [9]. PALSAR datasets were converted by the same software. It provides a convenient way to extract backscatter coefficients (sigma nought, in decibel) from JAXA CEOS format. Similar to those of NDVI, 75 pixels were selected in further assessment and model building.

Table 1. Random Forest Parameters

Parameters	AVNIR-2	PALSAR
Random Forest Options		
Number of Predictors	4	3
Number of Trees	100	100
Random Test Data Proportion	0.3	0.3
Subsample Proportion	0.5	0.5
Seed for Random Number Generator	1	1
Stopping Parameters		
Minimum Number of Cases	75	75
Minimum Number of Levels	10	10
Minimum Number in Child Nodes	5	5
Maximum Number of Nodes	100	100

The research employed supervised classification approach to obtain rice map. Sampling strategy was guided by planning data at block level. This was also enhanced by two field surveys in July-August 2009 and July 2010. Another data collection was taken in June 2011 to improve field datasets. Based on the collection, additional sample sets were also established. These samples were employed for testing classification rules. Decision tree was chosen as classification algorithm, mainly due to its easy-to-comprehend, flexible rule [10]. Random Forests [11] was particularly selected to aid the construction of classification rules. The algorithm has been tested for various applications with superior results [12, 13]. Following Random Forest specification was tested.

3. Results and Analysis

3.1. Fluctuation of NDVI Values

NDVI has been exploited on many biophysical observations from remotely sensed data. Using radiance data, NDVI values were retrieved and subsequently analyzed according to the field data (Figure 3).

On early ages (early tillering), observed NDVI tends to be around 0. This is due to the fact that fields are flooded by water and the rice is very small, which leads to strong contribution of non-vegetative components (water and soil) on the respective pixel. When rice grows, chlorophyll increases, which is therefore reflected by rising NDVI value. However, in certain periods, NDVI values are dropped significantly. From field observations, it was found that many blocks were severely infested. Two major infestations in research area were due to rats and golden apple snails (*Pomacea canaliculata*). All infested fields (Figure 4) were replaced by new seedlings. This leads to uneven appearance on particular fields.

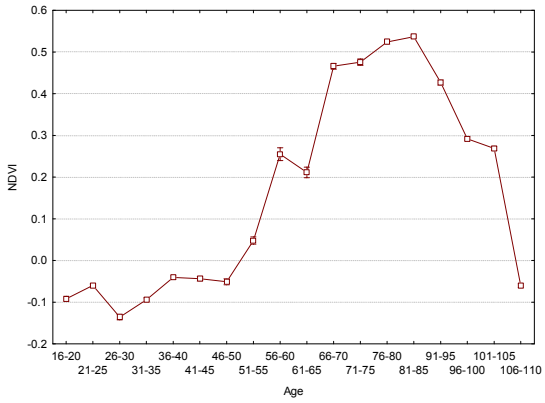

Figure 3. Observed NDVI over Ciherang Cultivar

Figure 4. Infestation by Rats

NDVI increases during vegetative phase until early generative (heading) stage. At this point, NDVI starts to decrease. As shown in Figure 3, NDVI of Ciherang variety reaches the peak at about 90 days. This result approves a previous study by means of time series MODIS observation in the same site [14].

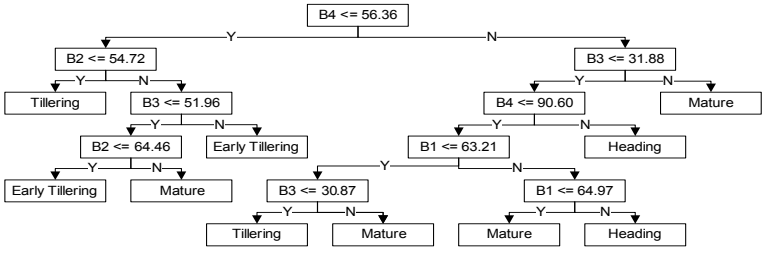

Figure 5. Decision Tree for AVNIR-2 Data

NDVI curve indicates that at least four growth stages are visible. Those are early tillering (less than 50 days), tillering (50-70), heading (71-90), and mature (more than 90). According to those classes, all pixels in the imagery were then classified exploiting Random Forest. Following figure shows a result of Random Forest decision tree, while its associated accuracy is presented in Table 2.

Table 2. Accuracy in Per Cent, Based on 30% Sample Pixels

	Classified			
Observed	Early Tillering	Tillering	Heading	Mature
Early Tillering	99	0	0	1
Tillering	3	96	0	1
Heading	0	18	65	17
Mature	3	1	1	96

As shown in Figure 5, band 4 of AVNIR-2 played in crucial role in the development of rules, and selected by the algorithm as the main stem. This is due to the sensitivity of the band (820.6 nm) to vegetation, which has been widely known on a variety of optical sensors. Band 1, which is often used to identify water bodies, was substantial as well, especially on the discrimination of heading and mature stages. Rice fields are drained during the maturity of rice. Meanwhile, the Red band (Band 3) is employed to separate tillering and mature paddies. Lower value of Band 3 indicates a considerable involvement of soil/water background, and therefore these values fit into tillering class.

Overall accuracy using AVNIR-2 data obtained in this experiment is reasonably good, as indicated in Table 2. However, it appears that heading is comparatively confused to tillering and mature stages. This is fairly understandable since the class has no significant features which influence distinctive spectral signature. NDVI pattern presented in Figure 3 also supports the argument, where heading is indicated by gentle slope, shortly before the peak (the end of vegetative phase). This also suggests that even Band 1 can be employed for discrimination of mature and heading, the bias remains considerably high.

3.2. Backscatter Coefficient

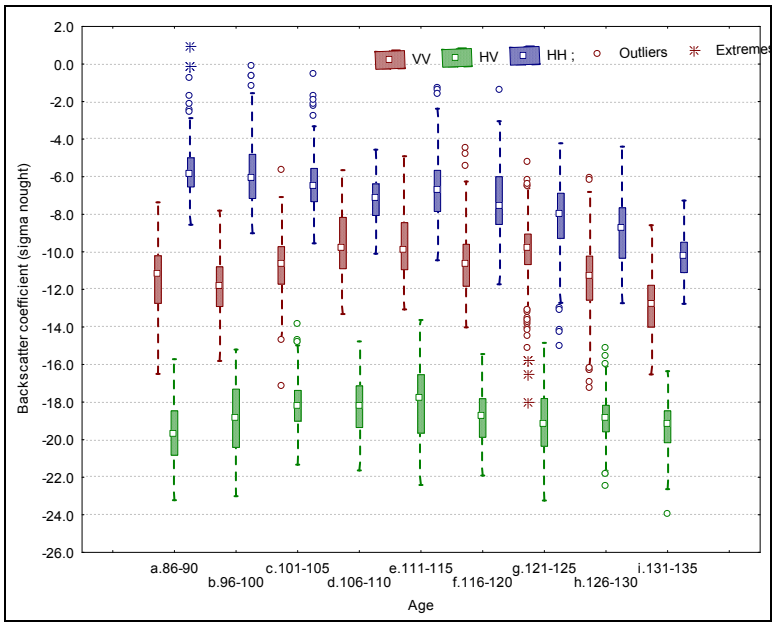

Figure 6. Backscatter Patterns of Rice Phenology. Prolonged rice planting was due to extensive replanting in 2007.

Backscatter intensities have been employed to observe and to model interaction between radar signals and surface materials. This research focuses on the observation of sigma-nought among various ages (after transplanting). Due to monostatic nature of PALSAR sensor, VH data can be omitted as a consequence of the reciprocity theorem. Following figure shows variability of backscatter data extracted from combined 2007 and 2009 PLR data.

As shown, HH has the highest backscatter coefficients. On HH polarization, higher amplification of backscatter is due to strong contribution of double bounce scattering mechanism. L-band HH signals are capable to penetrate canopy layer and therefore interact with soil background. Since the soil is usually flooded during peak vegetative stage, signals consecutively interact with soil and the rice.

Higher backscatter contribution of HH was also reported by numerous researchers [6-7]. At the early tillering, Wang *et al*. [7] reported low backscatter returns due to sparse vegetation, and therefore, overall scattering is dominated by specular propagation. This stage was missed in the research due to lack of PLR data and most blocks were in heading or pre-harvest stages. However, it appears that our results are in line and complementary to previous findings [7], with similar absolute value of sigma-nought. Declining SAR returns at L-band were also reported [15]. Structural property, i.e. drying leaves, was reported as the main cause of the decline [7].

Amplification of HH was reported in mechanical-based planting system in Japan [16] and in China [6]. Although the Sang Hyang Seri did not implement fully mechanical system, field observation discovered that space between rice was regular (squared, with 20 cm space between plants). This regular space can create the Bragg scattering, which observable in high percentage of HH signals.

Figure 7. Regular Pattern of Rice Planting

Specifically for VV polarization, Figure 4 shows high variation of SAR backscatters. Previously, VV was demonstrated least useful for rice monitoring [15]. This is also reflected by our results. It appears that disagreement remains in fluctuated backscatter coefficients during rice growth, especially at C-band. Durden *et al*. [17], for instance, found that microwave returns tended to decrease during growing period at C-band AIRSAR. However, Tsang *et al*. [18] model indicated that there is an increase of SAR backscatters of ERS-1 VV polarization.

Low returns of SAR signals at HV are primarily due to complex propagation of signals in vegetative cover. This was extensively reported by numerous papers, including Santoro *et al*. [19]. We found that HV pattern of Ciherang cultivar is quite similar to Ling *et al*. [6] observation in East China using dual-polarized PALSAR. HV pattern is also comparable to Wang et al. [7] findings.

PALSAR data span was quite different than AVNIR-2. This created a condition where PALSAR data contain only heading and mature phases. Using Random Forest, a simple separation rule between heading and mature was established (Figure 8). It is interesting that VV polarization was selected by Random Forest algorithm, even assessment of backscatter showed higher preference of HH. This is probably due to the effect of grouping rice age into growth class (heading and mature). Another source of the bias would be parameter selection,

which is subject for further assessment. Due to simple separation, it is obvious to see that the overall accuracy tends to be higher (Table 3). Similar to those in AVNIR-2, heading was harder to detect in all PALSAR PLR data. Most of pixels belong to heading was reportedly misclassified into mature class.

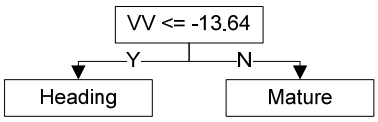

Figure 8. Decision Tree for PALSAR Linear Polarization

Table 3. Confusion Matrix Based on 30% Samples

	Classified	
Observed	Heading	Mature
Heading	65	17
Mature	1	96

4. Conclusion

This research demonstrates the capabilities of ALOS sensors to retrieve invaluable information on rice fields. It was shown that growth disturbance, especially in transplanting and early vegetative stages, was somewhat visible from NDVI plot. Vegetative stage of Ciherang cultivar was peaked at about 90 days, similar to previous observation using time series MODIS data. Classification by means of Random Forest on AVNIR-2 data produced substantially high accuracy. However, improvements are still required since heading stage was confused with tillering and mature stages. The research was unable to collect PLR data covering full phase of rice production. In this case, early tillering and tillering phases were missing. Therefore, full conclusion cannot be drawn using solely available PLR data. However, it is interesting to observe that difficulties to discriminate heading stage are quite similar on both AVNIR-2 and PLR data.

These all suggest that AVNIR-2 and PALSAR fully polarimetric datasets are useful to monitor various rice growths. Nonetheless, several issues need to be addressed. Availability has been a primary obstacle for fully polarimetric SAR. It is suggested that regular fully polarimetric acquisition cycle needs to be revised to accommodate a thorough rice field observation. Acquisitions in a couple of weeks after mid-season of rainy monsoon (about December-January at the test site) are suggested to examine applicability of SAR data for estimating rice productivity.

Acknowledgements

This research was supported by JAXA and RESTEC, Japan. Additional funding was provided by Indonesian Ministry of Agriculture through KKP3T project. The authors acknowledge substantial assistance of Mr. Masatoshi Kamei of RESTEC and Mrs. Ita Carolita of LAPAN who managed image acquisition. We are grateful to our Japanese fellows for their enthusiasm and support during the research. We thank our students at the Department of Soil Science and Land Resources, Bogor Agricultural University for their assistance during the research.

References

[1] Van Valkenberg S. Java: The Economic Geography of A Tropical Island. *Geographical Review*. 1925; 15(4): 563-583.
[2] Panuju DR, Mizuno K, Trisasongko BH. The Dynamics of Rice Production in Indonesia 1961-2009. *Journal of the Saudi Society of Agricultural Sciences*. 2013; 12(1): 27-37.

[3] Haldar D, Patnaik C. Synergistic Use of Multi-temporal Radarsat SAR and AWiFS Data for Rabi Rice Identification. *Journal of Indian Society of Remote Sensing*. 2010; 38(1): 153-160.
[4] Chen J, Lin H, Huang C, Fang C. The Relationship between the Leaf Area Index (LAI) of Rice and the C-band SAR Vertical/Horizontal (VV/HH) Polarization Ratio. *International Journal of Remote Sensing*. 2009; 30(8): 2149-2154.
[5] Ishitsuka N. *Observation of Japanese Paddy Fields Using PALSAR Data*. IEEE International Geoscience and Remote Sensing Symposium. Vancouver, Canada. 2011: 1938-1941.
[6] Ling F, Li Z, Chen E, Tian X, Bai L, Wang F. *Rice Areas Mapping Using ALOS PALSAR FBD Data Considering the Bragg Scattering in L-band SAR Images of Rice Fields*. IEEE International Geoscience and Remote Sensing Symposium. Honolulu, USA. 2010: 1461-1464.
[7] Wang C, Wu J, Zhang Y, Pan G, Qi J, Salas WA. Characterizing L-band Scattering of Paddy Rice in Southeast China with Radiative Transfer Model and Multitemporal ALOS/PALSAR Imagery. *IEEE Transactions on Geoscience and Remote Sensing*. 2009; 47(4): 988-998.
[8] Lillesand TM, Kiefer RW, Chipman JW. Remote Sensing and Image Interpretation. Fifth Edition. New York: John Wiley & Sons. 2005: 546-550.
[9] Shimada M, Isoguchi O, Tadono T, Isono K. PALSAR Radiometric and Geometric Calibration. *IEEE Transactions on Geoscience and Remote Sensing*. 2009; 47(12): 3915-3932.
[10] Friedl MA, Brodley CE. Decision Tree Classification of Land Cover from Remotely Sensed Data. *Remote Sensing of Environment*. 1997; 61(3): 399-409.
[11] Breiman L. Random Forests. *Machine Learning*. 2001; 45(1): 5-32.
[12] Zhou L, Wang H. Loan Default Prediction on Large Imbalanced Data Using Random Forests. *TELKOMNIKA Indonesian Journal of Electrical Engineering*. 2012; 10(6): 1519-1525.
[13] Myint SH. Overload Pattern Classification for Server Overload Detection. *International Journal of Information & Network Security*. 2013; 2(3): 260-266.
[14] Panuju DR, Heidina F, Trisasongko BH, Tjahjono B, Kasno A, Syafril AHA. Variasi Nilai Indeks Vegetasi MODIS pada Siklus Pertumbuhan Padi. *Jurnal Ilmiah Geomatika*. 2009; 15: 9-16. (in Indonesian).
[15] Inoue Y, Kurosu T, Maeno H, Uratsuka S, Kozu T, Dabrowska-Zielinska K, Qi J. Season-long Daily Measurements of Multifrequency (Ka, Ku, X, C, and L) and Full-Polarization Backscatter Signatures over Paddy Rice Field and their Relationship with Biological Variables. *Remote Sensing of Environment*. 2002; 81(2-3): 194-204.
[16] Ouchi K, Wang H, Ishitsuka N, Saito G, Mohri K. On the Bragg Scattering Observed in L-band Synthetic Aperture Radar Images of Flooded Rice Fields. *IEICE Transactions on Communication*. 2006; E89-B(8): 2218-2225.
[17] Durden SL, Morrissey LA, Livingston GP. Microwave Backscatter and Attenuation Dependence on Leaf Area Index for Flooded Rice Fields. *IEEE Transactions on Geoscience and Remote Sensing*. 1995; 33(3): 807-810.
[18] Tsang L, Kong JA, Ding K, Ao CO. Scattering of Electromagnetic Waves 2: Numerical Simulation, New York: Wiley Interscience. 2001: 685-692.
[19] Santoro M, Fransson JES, Eriksson LEB, Magnusson M, Ulander LMH, Olsson H. Signatures of ALOS PALSAR L-band Backscatter in Swedish Forest. *IEEE Transactions on Geoscience and Remote Sensing*. 2009; 47(12): 4001-4019